GEOLOGICA CARPATHICA, FEBRUARY 2008, 59, 1, 19–30

Thermal evolution of the Žiar Mountains basement (Inner Western Carpathians, Slovakia) constrained by fission track data

MARTIN DANIŠÍK[1,✉], MILAN KOHÚT[2], ISTVÁN DUNKL[3] and WOLFGANG FRISCH[1]

[1]University of Tübingen, Institute of Geosciences, Sigwartstrasse 10, D-72076 Tübingen, Germany; ✉martin.danisik@uni-tuebingen.de
[2]Dionýz Štúr State Institute of Geology, Mlynská dolina 1, 817 04 Bratislava, Slovak Republic; milan.kohut@geology.sk
[3]Geoscience Center Göttingen, Sedimentology and Environmental Geology, Goldschmidtstrasse 3, D-37077 Göttingen, Germany

(Manuscript received February 13, 2007; accepted in revised form June 13, 2007)

Abstract: Thermal evolution of the Žiar Mts was studied using zircon and apatite fission track (ZFT and AFT) thermochronology applied to basement and sedimentary rocks. Basement samples from the Tatric Unit of the Inner Western Carpathians (IWC) yielded cooling ZFT ages in the range from 109 ± 5.9 to 92.1 ± 5.3 Ma and apparent AFT ages between 33.7 ± 2.7 and 24.4 ± 1.7 Ma. Paleogene sediments of the Central Carpathian Paleogene Basin (CCPB) yielded apparent AFT ages of 73.2 ± 2.7 and 49.6 ± 1.8 Ma. ZFT data show that during early Late Cretaceous thrusting the crystalline basement was buried by a nappe pile to crustal depths with temperatures between 210 and 310 °C, where the crystalline core was metamorphosed at anchizonal conditions. AFT data revealed a complex thermal evolution, implying that after nappe stacking and metamorphism the basement was exhumed to the surface and that it was buried beneath a thick pile of sediments of the CCPB. The CCPB was inverted and the basement finally exhumed in the Late Oligocene to Early Miocene. The AFT system in the basement and CCPB samples record also a distinct, Middle Miocene thermal event, related to the increased heat flow induced by upwelling of hot mantle material and related volcanic activity. Our data support the hypothesis that the study area was part of a large CCPB basin and contradict the widely accepted assumption that the Variscan crystalline core of the Žiar Mts lacks an Alpine metamorphic overprint.

Key words: Cretaceous and Tertiary, Western Carpathians, Žiar Mts, burial and exhumation, thermochronology, thermal modeling, fission track dating.

1. Introduction

The Western Carpathians are the northernmost, W-trending branch of the Alpine orogenic belt, linked to the Eastern Alps in the west and to the Eastern Carpathians in the east. They are part of a complexly curved orogenic belt, which originated from the collisional tectonics and escape of fragments of the Adriatic (Apulian) plate with the European foreland during Oligocene to Miocene times (e.g. Maheľ 1986; Ratschbacher et al. 1991a,b). They are divided into two principal tectonic domains [Outer (OWC) and Inner Western Carpathians (IWC)] separated by the Pieniny Klippen Belt (PKB; Fig. 1A; e.g. Biely 1989). The IWC are formed by pre-Tertiary formations (Variscan crystalline basement with Upper Paleozoic–Mesozoic cover, overlain by Mesozoic nappes), exposed beneath the post-tectonic Paleogene and Neogene sedimentary and Miocene to Quaternary volcano-sedimentary covers. Crystalline basement is exposed in several mountain ranges that form three structural zones (from external to internal regions: the Tatric, Veporic and Gemeric belts), arranged roughly parallel to the PKB (Plašienka et al. 1997).

The geodynamic evolution of the IWC during Paleogene times is not sufficiently understood. Basically, two contrasting models are proposed: Kováč et al. (1994) argued from stratigraphic, fission track and paleomagnetic data that during the Eocene some of the Tatric crystalline bodies of the IWC were uplifted in the course of collision between the Adriatic and the European plate. In contrast, based on the sedimentological, fission track and thermal modeling data, Kázmér et al. (2003) and Danišík et al. (2004) pointed out that the Paleogene forearc basin (Central Carpathian Paleogene Basin — CCPB) played a more important role in the geodynamic evolution of the IWC than previously thought. These authors proposed that during the Eocene period the pre-Tertiary formations of the IWC underwent maximum burial when they were overburdened by a thick pile of CCPB sediments.

In order to address this issue, we used zircon and apatite fission track (ZFT and AFT) thermochronology, because this technique can be efficiently used to decipher the thermal evolution of rocks in the uppermost crust (e.g. Wagner et al. 1977; Gleadow & Fitzgerald 1987) and to estimate the amount of overburden (e.g. Gleadow et al. 1983; Naeser et al. 1989). We targeted the small mountain range of the Žiar Mts in the IWC (Fig. 1A) due to a number of advantageous features provided by this area: (i) as compared to the other core mountains of the IWC, the geological structure of the Žiar Mts is simple — pre-Tertiary formations are formed mainly by a deeply eroded Variscan granitic pluton exposed in the central part of the range, whereas the Mesozoic sequences are sparsely preserved in the northern and southern marginal parts; (ii) remnants of the CCPB sediments occur in close vicinity to the

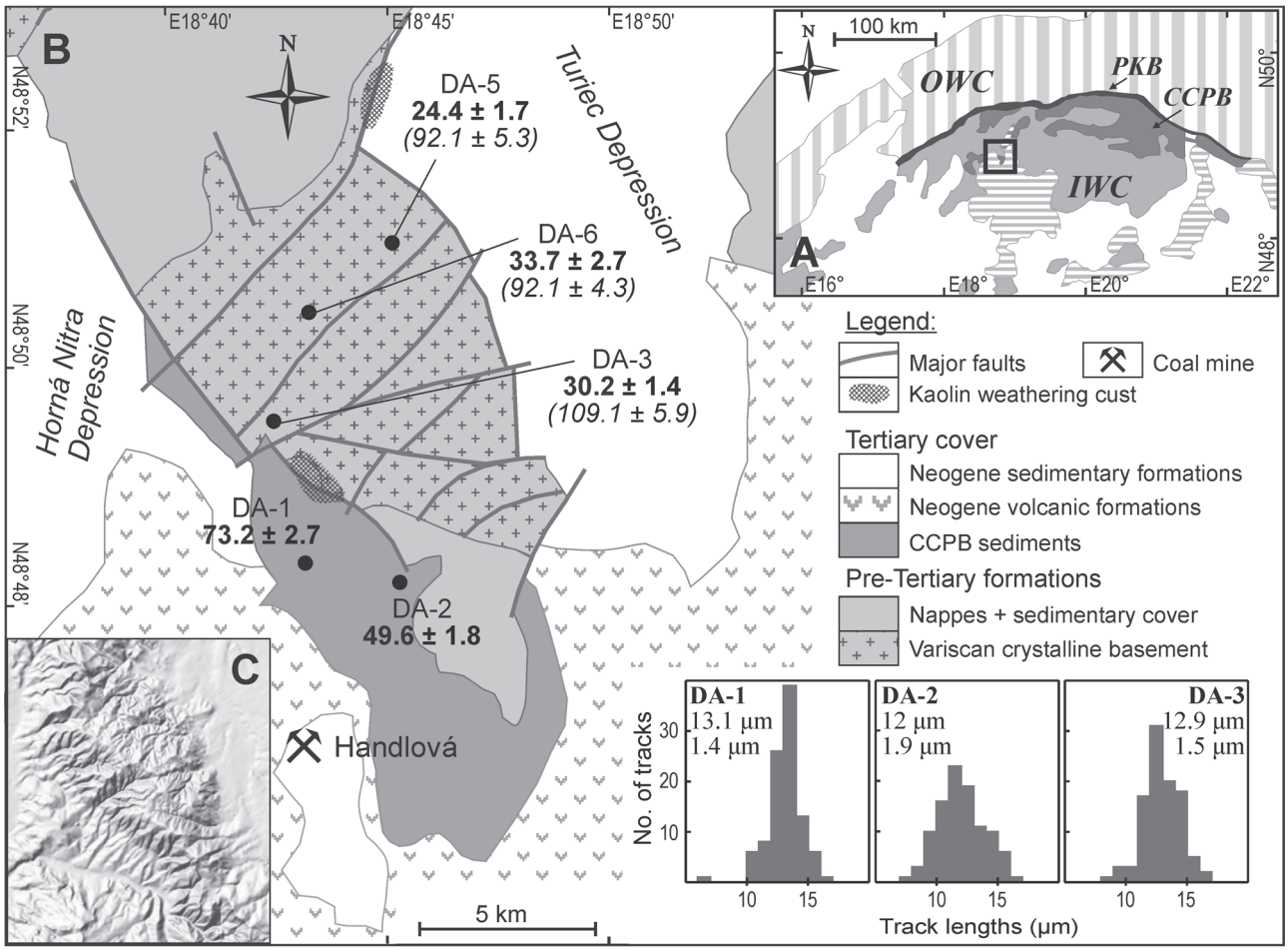

Fig. 1. A — Simplified geological map of the Western Carpathians with location of the study area (black rectangle): OWC — Outer Western Carpathians (vertical hatching); IWC — Inner Western Carpathians (pre-Tertiary formations are depicted in light grey); PKB — Pieniny Klippen Belt (black); CCPB — Central Carpathian Paleogene Basin (dark grey); Neogene volcanic formations are depicted by horizontal hatching; Neogene and Quaternary sedimentary formations are depicted in white. **B** — Geological sketch map of the Žiar Mts and surrounding areas (modified after Kohút 1999; Lexa et al. 2000) with location of the samples (black dots) and fission track data. The text beside the dots shows, from top to bottom, the sample code, the central apatite FT age with 1σ error in Ma (bold) and the central zircon FT age with 1σ error (italic in brackets). Measured track length distributions are presented in the bottom right. The numbers on histograms give, from top to bottom, the sample code, the mean track length and the standard deviation of the track length distribution. **C** — Shaded DEM of the Žiar Mts.

crystalline basement and provide an excellent opportunity to constrain the original thickness of the eroded cover; (iii) geological records of erosion and uplift events are relatively well preserved; (iv) the crystalline basement of the Žiar Mts is traditionally regarded to be exhumed and uplifted during the Eocene (e.g. Kováč et al. 1994; Hók et al. 1995, 1998), which would make it one of the earliest emerged crystalline complexes of the Tatric belt; (v) owing to the "inherited information" of its assumed geodynamic stability, the crystalline basement of the Žiar Mts was considered to be promising from the viewpoint of finding a geological structure for hosting radioactive waste in a deep repository (e.g. Kováčiková et al. 1995).

In this study, we aim to investigate the thermal history of the samples taken from the crystalline basement and also from sediments of the CCPB in order to better understand the final cooling evolution of the Žiar Mts. Our FT data enable us to present a new interpretation of the thermal history of the Žiar Mts and will have implications for the geodynamic development of the IWC.

For this purpose we first briefly review the geological setting of the study area and the geochronological data and briefly explain the potential of the FT method. Then we present and interpret our data and discuss their inferences with respect to the thermotectonic evolution of the Žiar Mts and to the geodynamic evolution of the IWC as a whole.

2. Geological setting

The Žiar Mts is one of the smallest core mountains in the Tatric Unit of the IWC situated in Central Slovakia (Fig. 1B). The mountains form an asymmetric, NW-trending and NE dipping horst structure, flanked by two Neogene grabens (Fig. 1C).

The pre-Tertiary formations of the mountains were arranged during Late Cretaceous (Turonian) nappe stacking (Plašienka 1997) and consist of three tectonic units, from bottom to top: Tatricum–Variscan crystalline basement with sedimentary cover and two Mesozoic cover units — Fatricum and Hronicum (e.g. Maheľ 1986; Plašienka et al. 1997). The crystalline basement of the Tatricum is built up of various unmetamorphosed granitoids (e.g. Plašienka et al. 1997), related to the Variscan orogeny (Kráľ & Štarková 1995). The Mesozoic cover units consist predominantly of carbonates, their occurrences are restricted to the northwestern and southeastern margin of the horst mountains. The relics of a kaolin weathering crust of Oligocene?–Middle Miocene age preserved in situ on the top of the granitoids in the northern part of the mountains (Fig. 1B) indicate that the basement must have experienced a period of tectonic quiescence and formed a peneplain favourable for supergene kaolinization (Kraus 1989). The minimum age of the kaolinization is not exactly known, since it was indirectly assessed from available AFT data (unpublished data of J. Kráľ, see Table 26 in Kraus 1989). The horst mountains are cut by SW-NE oriented faults into several blocks without significant vertical displacement (e.g. Nemčok & Lexa 1990).

The post-tectonic cover is represented by sediments of the CCPB and by sedimentary and volcanic rocks of Neogene age. Sediments of the CCPB are exposed only along the southern margin of the horst and have a maximum thickness of a few hundred meters (Gross et al. 1984). Boreholes, however, proved the presence of an up to 1000 m thick column beneath the Neogene deposits in both adjacent intramontane depressions (Fendek et al. 1990). The sequence transgressively overlies the pre-Tertiary formations and consists of: (i) Lutetian basal conglomerates and breccias, overlain by limestones and marls (Borové Formation), pointing to syn-sedimentary tectonic activity followed by subsidence; (ii) Priabonian to Rupelian flysch — shales, siltstones and sandstones (Huty and Zuberec Formations), indicating continued subsidence; (iii) the sequence ends with locally preserved Rupelian to Aquitanian sandstones and shales (Biely Potok Formation), which unconformably overlie the Huty Formation. Due to severe erosion and tectonic activity during the Neogene, the original thickness of the Paleogene sequence is not exactly known.

Neogene sedimentary formations are exposed in two fault-bounded intramontane depressions (Turiec Depression in the east, Horná Nitra Depression in the west). They transgressively overlie all pre-Neogene formations and reach a maximum thickness of more than 1000 m (Fendek et al. 1990; Hók et al. 1995, 1998). In general, they consist of Eggenburgian to Quaternary shales, sandstones, conglomerates and breccias, often interbedded by volcanic and volcaniclastic rocks (for details see Hók et al. 1995, 1998).

The Neogene volcanic formations (lava flows, tuffs, pyroclastic and volcanic breccias) are subduction-related calc-alkaline rocks of Langhian to Serravalian age (ca. 16–12 Ma; e.g. Lexa & Konečný 1998 and references therein). They form the remnants of stratovolcanoes in the southeastern part of the study area and, as mentioned above, can also be found in the sequences of neighbouring Neogene depressions.

2.1 Older geochronological and thermochronological data

There is general lack of geochronological data available from the Žiar Mts, with the exception of Ar/Ar ages on muscovite and biotite from the granitic rocks, yielding 338.1 ± 1.7 and 287 ± 1.3 Ma, respectively (Kráľ & Štarková 1995). These ages are interpreted as cooling ages of the granitic massif after emplacement during the Variscan orogeny.

Actually the only thermochronological data can be found in the work of Kováč et al. (1994), who reported four apatite fission track ages from the granitic pluton, ranging from 52 ± 7 to 46 ± 5 Ma. However, these data lack important information such as exact sample location and, even more important, track length data, which are critical for proper interpretation of the ages (see section 3). The authors interpret their ages in terms of the closure temperature concept, correlating the age to the passage of the ~110 °C isotherm (Dodson 1973; Wagner & Van den haute 1992). In conclusion they found evidence for Eocene uplift and denudation of the crystalline basement and related it to the Eocene compressional event.

3. Fission track dating method

Fission track analysis is a standard thermochronological technique based on the spontaneous nuclear fission of ^{238}U, which produces linear trails of radiation damage (fission tracks) in the crystal lattice of U-bearing minerals. The principle of fission track dating relies on the constant production rate of fission tracks through time (Price & Walker 1963). The fission track age is determined from the ratio of the parent isotope (^{238}U measured via fission tracks induced by thermal neutron irradiation procedure) and daughter products (spontaneous fission tracks counted per unit area observed on the polished surface of a mineral). The technique can be applied to a variety of U-bearing minerals, apatite and zircon being the best studied and most common. Owing to the phenomenon of fission track annealing, measured fission track ages need not necessarily be related to the age of rock/mineral formation or a distinct geological event.

Fission tracks are stable over geological time, but only at relatively low temperatures (≤ ~ 60 °C in apatite, ≤ ~ 210 °C in zircons). At elevated temperatures in the so-called partial annealing zone (PAZ), the fission tracks are gradually repaired, or "annealed". At temperatures above ~120 °C in apatite and ~290 °C in zircon they are totally annealed in a short time (e.g. Zaun & Wagner 1985; Hurford 1986; Wagner & Van den haute 1992).

In case of apatite the fission tracks are approximately 16 μm long and, depending on the time spent in the PAZ, they are progressively shortened to different extents. The

resulting length distribution of spontaneous tracks is thus a direct record of the thermal history experienced by the sample. Age and length distribution therefore enable a quantitative reconstruction of the thermal history of a sample (Gleadow et al. 1986a,b) by means of sophisticated numerical annealing models (e.g. Laslett et al. 1987; Green et al. 1989; Crowley et al. 1991; Ketcham et al. 1999).

As mentioned above, the measured FT age alone directly refers to a geological event only in special cases. Depending on the nature of the thermal history experienced, there are essentially three different kinds of "ages" recognized in the thermochronological system: formation ages, cooling ages and apparent ages. The meaning of these can be straightforwardly resolved from the track length distributions (see Fig. 2).

(i) "Formation" (or "event") ages are typical of volcanic rocks, when they rapidly cooled through the PAZ (Fig. 2A). The resulting track length distribution is unimodal and narrow (as shown by standard deviations — SD — of $<1.5\,\mu m$) with long mean track length (MTL $>14\,\mu m$).

(ii) If a sample undergoes slow and monotonous cooling through the PAZ (Fig. 2B), the track length distribution is unimodal and broader (SD $>1.5\,\mu m$) and the MTL shorter ($<14\,\mu m$). The age is described as a "cooling" age. This kind of cooling is common in basement rocks with a simple cooling history. An important point here is that the observed age is not related to a distinct geological event but the cumulative effect of the slow passage of the rock through the PAZ.

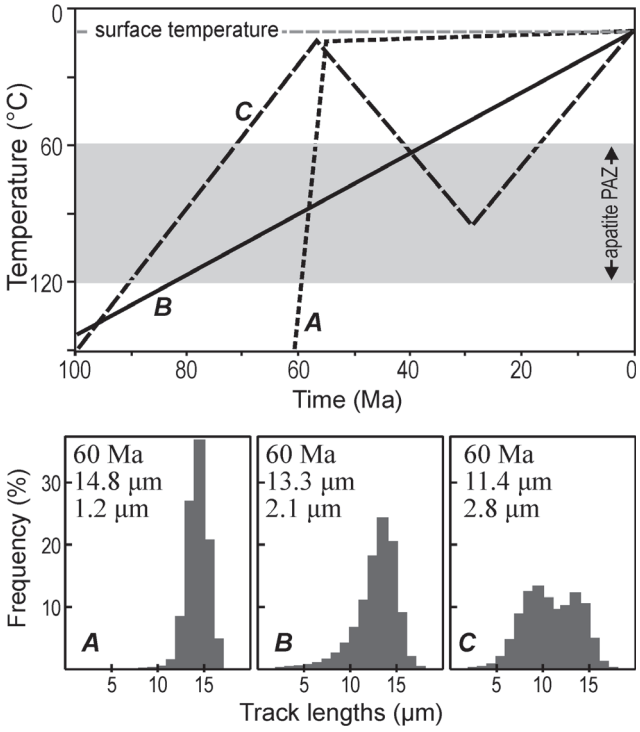

Fig. 2. Three different cooling paths of hypothetical samples (upper panel: **A** — rapid cooling resulting in formation age; **B** — slow steady cooling resulting in cooling age; **C** — complex cooling with thermal overprint resulting in apparent age) and corresponding track length distributions (lower panels). The fission track results are calculated using the model of Ketcham et al. (1999) with the initial track length of 16.1 µm. The numbers on the track length histograms give, from top to bottom, the calculated fission track age, the mean track length and the standard deviation of the track length distribution. Note that inspite of markedly different cooling styles, the resulting age is the same (60 Ma) in all three cases.

(iii) The third case shows a complex thermal history with a period of reheating into the PAZ (Fig. 2C), which is a common case in rocks buried by sediments. The track length distribution in a such case is frequently bimodal and broad (SD $>2.5\,\mu m$) with a short MTL ($<13\,\mu m$). The age is a combination of two components and described as an "apparent" (or "mixed") age. Like in the previous case, the age has no direct significance in terms of the timing of a geological event. However, even in this case it is possible to reveal the magnitude and timing of cooling and reheating periods by thermal modeling.

In conclusion, without information on track length distribution the true meaning of the AFT ages cannot be unraveled. In order to provide a clear picture of the meaning of AFT data, the data are commonly presented as a combination of measured ages, track length distributions (histograms with MTL and SD) and modeled time-temperature paths or envelopes of possible solutions.

The precise usage of terminology is essential in understanding FT data. In the past thermochronological data were often incorrectly interpreted in terms of "uplift" or "uplift rates". Therefore we begin with definitions of terms used throughout this paper. We follow the works of England & Molnar (1990), Ring et al. (1999), Stüwe & Barr (1998), and Stüwe (2002), and use the following terminology:

The terms **uplift** (motion upwards) and **subsidence** (motion downwards) describe vertical motion relative to a fixed reference level (e.g. relative to the geoid, sea level, or other reference points). Two kinds of uplift are distinguished: (i) surface uplift — vertical motion the Earth's surface; and (ii) rock uplift — vertical motion of rock. Both terms should always be used together with specification of the reference level. Surface uplift can be directly determined for instance from paleobotany, paleoaltimetry, paleoclimatology or GPS data. Both types of uplift can be indirectly determined from sediments in the surrounding basins. However, neither of these motions can be interpreted from thermochronology. In this study, due to lack of data, the term uplift is only used for rock uplift, with the erosion base level as a reference level.

The terms **exhumation** (motion towards the surface) and **burial** (motion away from the surface) describe vertical displacement of rocks relative to the Earth's surface. They can be indirectly determined for instance from geobarometry, geochronology, or thermochronology, when the thermal structure of the crust as defined by isotherms can be reconstructed with sufficient accuracy. Thermochronological data in fact do record the motion of rock relative to the isotherms, which form the reference frame. Therefore they can be interpreted in terms of exhumation or burial, but cannot tell anything about uplift

Table 1: Apatite fission track data[a].

Sample code	lat-long (°)/WGS84 lat	long	Altitude (m)	Tectonic unit	Formation/ stratigraphic age	Petrography	N	ρ_s	N_s	ρ_i	N_i	ρ_d	N_d	$P(\chi^2)$ (%)	Age (Ma)	± 1σ (Ma)	MTL (μm)	SD (μm)	SE (μm)	N (L)	Dpar (μm)
DA-1	48.773	18.719	360	CCPB	Chattian–Aquitanian ~26–20 Ma	sandstone	50	8.151	2223	9.449	2577	5.286	3675	99.9	73.2	2.7	13.1	1.4	0.1	100	1.6
DA-2	48.771	18.761	400	CCPB	Rupellian–Chattian ~33–26 Ma	sandstone	50	8.763	1974	15.547	3502	5.474	3675	93.2	49.6	1.8	12	1.9	0.2	100	1.6
DA-3	48.812	18.714	440	crystalline basement	Carboniferous	granite	25	5.541	902	16.641	2709	5.624	3675	47.5	30.2	1.4	12.9	1.5	0.1	100	1.6
DA-5	48.850	18.757	510	crystalline basement	Carboniferous	granite	30	2.878	310	11.260	1213	5.924	3675	96.5	24.4	1.7					
DA-6	48.836	18.727	378	crystalline basement	Carboniferous	granite	30	1.955	294	5.599	842	6.186	3675	88.1	33.7	2.7					

[a] **N** — number of dated apatite crystals; ρ_s **(ρ_i)** — spontaneous (induced) track densities ($\times 10^5$ tracks/cm^2); N_s **(N_i)** — number of counted spontaneous (induced) tracks; ρ_d — dosimeter track density ($\times 10^5$ tracks/cm^2); N_d — number of tracks counted on dosimeter; $P(\chi^2)$ — probability obtaining Chi-square value (χ^2) for n degree of freedom (where n = No. of crystals – 1); **Age ± 1σ** — central age ± 1 standard error (Galbraith & Laslett 1993); **MTL** — mean track length; **SE** — standard error of mean track length; **SD** — standard deviation of track length distribution; **N (L)** — number of horizontal confined tracks measured; **Dpar** — average etch pit diameter of fission tracks. Ages were calculated using zeta calibration method (Hurford & Green 1983), glass dosimeter CN-5, and zeta value of 322.7 ± 5.3 year/cm^2.

movements with the exception of the special case when surface uplift equals zero.

4. Sampling and analytical procedure

The sampling campaign focused primarily on the crystalline basement and sediments of the CCPB (for locations and coordinates see Fig. 1B and Table 1). All but one of the samples were taken from surface outcrops; sample DA-6 was collected in the drill core from the exploratory borehole RAO-4 in the central part of the mountains (Kohút et al. 2004), from the depth of 43 m below surface. The basement samples were collected along a NNE-trending transect crossing the central part of the crystalline core. Two samples of the CCPB sediments were collected from the southern foothill of the mountains. Sample DA-1 is a sandstone of the Biely Potok Formation (Šimon et al. 1997), which was dated as Chattian–Aquitanian by palynomorphs (~26–20 Ma; Šimon et al. 1994). Sample DA-2 is a sandstone attributed to the Huty-Zuberec Formations; the age is indirectly determined by the overlapping rocks as Upper Oligocene (Rupelian?) (~33–26 Ma; Šimon et al. 1997).

The analytical procedure used for FT analysis can be found in the Appendix.

5. Results

AFT ages were successfully determined on 5, ZFT ages on 3 samples (Tables 1 and 2, Fig. 1B). All samples passed the chi-square test at the 95 % confidence interval. The FT ages are reported as central ages with 1σ errors. ZFT ages were determined on basement samples only; they are 109.1 ± 5.9 (DA-3), 92.1 ± 4.3 (DA-6), and 92.1 ± 5.3 (DA-5) Ma. AFT ages are in the range from 73.2 ± 2.7 (DA-1) to 24.4 ± 1.7 Ma (DA-5), no age-elevation correlation was observed. Track length distributions were measured on 3 apatite samples (DA-1, DA-2, DA-3; Table 1, Fig. 1B). All samples are characterized by unimodal, fairly broad track length distributions [SD between 1.4 (DA-1) and 1.9 μm (DA-2)] with short MTL [MTL between 12.0 μm (DA-2) and 13.1 μm (DA-1)]. In all samples Dpar values (Dpar — etch pit diameter of fission tracks parallel to the crystallographic c-axis at the polished, etched, and analysed apatite surface; Crowley et al. 1991; Naeser 1992; Burtner et al. 1994) range from 1.5 to 1.7 μm (Table 1), pointing to a homogeneous composition of the apatites close to the fluorapatite end-member (Ketcham et al. 1999).

6. Interpretation and discussion

6.1 ZFT data

ZFT data from the basement show similar central ages in the range of ~110–90 Ma. From the AFT data (see below) and the zircon single grain age distribution [$P(\chi^2) > 95$ %]

Table 2: Zircon fission track data[a].

Sample code	N	ρ_s	N_s	ρ_i	N_i	ρ_d	N_d	$P(\chi^2)$ (%)	Age (Ma)	± 1σ (Ma)
DA-3	25	133.764	1504	49.539	557	6.591	6973	81.5	109.1	5.9
DA-5	25	92.452	1155	40.343	504	6.551	6973	97.5	92.1	5.3
DA-6	26	102.176	1846	44.668	807	6.561	6973	100.0	92.1	4.3

[a] N — number of dated zircon crystals; ρ_s (ρ_i) — spontaneous (induced) track densities ($\times 10^5$ tracks/cm^2); N_s (N_i) — number of counted spontaneous (induced) tracks; ρ_d — dosimeter track density ($\times 10^5$ tracks/cm^2); N_d — number of tracks counted on dosimeter; $P(\chi^2)$ – probability obtaining Chi-square value (χ^2) for n degree of freedom (where n = No. of crystals – 1); Age ± 1σ — central age ±1 standard error (Galbraith & Laslett 1993). Ages were calculated using zeta calibration method (Hurford & Green 1983), glass dosimeter CN-2, and zeta value of 123.6 ± 2.1 year/cm^2.

we consider the ages not to be rejuvenated during the Tertiary. The ages can be interpreted in two ways: (i) as cooling ages — recording the cooling of the basement following the thermal peak of metamorphism; or (ii) they can directly document the thermal peak of metamorphism. During metamorphism, the basement reached temperature conditions sufficient to fully reset the ZFT system (>210 °C). But, the maximum temperature must have been less than ~310 °C, so the Ar/Ar system in micas was not fully reset, as indicated by Ar/Ar ages of 338.1 ± 1.7 and 287 ± 1.3 Ma (Kráľ & Štarková 1995; closure temperature of Ar/Ar system in muscovite is ~350 °C and in biotite ~310 °C; Harrison et al. 1985; McDougall & Harrison 1988).

ZFT ages indicate that the basement experienced a thermal maximum during Albian to Turonian times. This coincides with the well-known period of thrusting in the Western Carpathians (Plašienka 1997). Thus we interpret the ZFT ages as related to the tectonic burial of the Tatric crystalline basement due to nappe stacking of the overlying Mesozoic nappes. The crystalline complex was buried to depths of ~8–10 km in order to explain the required temperatures using a gradient of ~30 °C/km. However, because it is likely that the burial occurred in the geodynamic context of an accretionary prism (see, e.g. Plašienka et al. 1997), a lower geothermal gradient may be expected and the basement might have reached greater depths.

It is widely accepted that the crystalline basement of the Žiar Mts has not experienced any metamorphism since Variscan times (e.g. Plašienka et al. 1997). However, our ZFT data show that the basement must have undergone at least very low-grade metamorphism. This conclusion is open to be corroborated by other kinds of data, such as illite crystallinity, maturation of organic material, fluid inclusions, stable isotope analysis, or higher-temperature geochronometry.

From the perspective of regional geology it is important to note that similar evolution was documented in the Eastern Alps, where the Austroalpine basement experienced metamorphism related to the Eo-Alpine orogeny (e.g. Frisch & Gawlick 2003) and some units were buried and metamorphosed even at HP/LT conditions. The peak of the metamorphism occurred at ~100 ± 10 Ma (e.g. Thöni & Jagoutz 1992; Thöni & Miller 1996), which exactly fits our data.

6.2 AFT data

6.2.1 Basement samples

All samples from the granitic basement yielded Oligocene AFT ages from 33.7 ± 2.7 (DA-6) to 24.4 ± 1.7 Ma (DA-5) and are thus younger than the Eocene AFT ages reported by Kováč et al. (1994; see section 2.1). The reason of this discrepancy lies, according to our opinion, in the dating technique used. Our data were measured by the external detector method (Gleadow 1981) using zeta calibration (Hurford & Green 1983), which became a standard technique in the early nineties. In contrast, the data reported by Kováč et al. (1994) were obtained by using the population dating technique (POP), which ruled in the seventies and eighties but since then has been abandoned. One of the advantages of the external detector technique is that it overcomes the problem of uncertainty about the value of the fission decay constant (λ_F), and it does not require knowledge of the absolute thermal neutron fluence (see Wagner & Van den haute 1992). In contrast, the POP technique requires precise knowledge of the absolute thermal neutron fluence, which is measured by gamma activity of metal detectors and is difficult to determine, and considers the decay constant of natural fission, which is not exactly known (the most frequently published values for λ_F range from 6.85 to 8.46×10^{-17} year^{-1}; Wagner & Van den haute 1992). Both parameters can, depending on the lambda value and metal detector used, introduce an uncertainty of up to 35 % into the age calculation (see e.g. Bigazzi 1981; Dunkl et al. 2003). The phenomenon of excessively old FT ages obtained by the POP method was also observed by other authors (e.g. Andriesen 1990; Dunkl et al. 2003), and there were attempts to recalculate the POP AFT ages by using different values of the decay constant. However, since the value of the decay constant used for calculation was not published by Kováč et al. (1994), the recalculation could not be done. We therefore do not consider the ages of these authors further on.

Track lengths were measured only in the sample DA-3. The sample yielded a unimodal, fairly broad (SD = 1.5 μm) distribution with short MTL (12.9 μm), typical of rocks, which experienced a complex thermal history and a long or repetitive stay within the apatite PAZ (Gleadow et al. 1986a,b). Therefore the AFT ages from the basement are interpreted as apparent ages without direct geological

meaning. The true meaning of the data can only be unraveled by thermal modeling (section 7).

6.2.2 Sedimentary samples

Samples from the Lower Miocene (Chattian–Aquitanian) and the Oligocene (Rupellian–Chattian) sandstones of the CCPB yielded AFT ages of 73.2 ± 2.7 Ma (DA-1) and 49.6 ± 1.8 Ma (DA-2), respectively. Similarly to the basement sample, track length distributions of both samples are unimodal and broad (SD = 1.4–1.9 μm) with short MTL (12 and 13.1 μm), indicating a complex thermal history (Gleadow et al. 1986a,b). Again, the AFT ages are apparent ages without direct geological meaning.

The AFT ages of both samples are clearly older than their stratigraphic age (~33–20 Ma). This means that the samples have not undergone thermal overprint after deposition, so the AFT thermochronometer has not been fully reset and possibly still records the information on the thermal history of the source area. There seems to be no principal difference in the single grain AFT ages: both samples passed the chi-square test ($P(\chi^2) > 90$ %) and show very low dispersion (see Fig. 3), indicating that the dated crystals form single age populations. This can be interpreted in two ways: (i) either the apatite grains have derived from source areas with cooling ages of ~73 and ~50 Ma, or (ii) all apatite crystals, coming originally from different sources and having diverse AFT ages, were partially reset after deposition and the AFT thermochronometer was set to a uniform value. We prefer the second option, because there are several sources of evidence indicating that the samples must have been thermally overprinted during the post-depositional period. We will develop this idea in the next section.

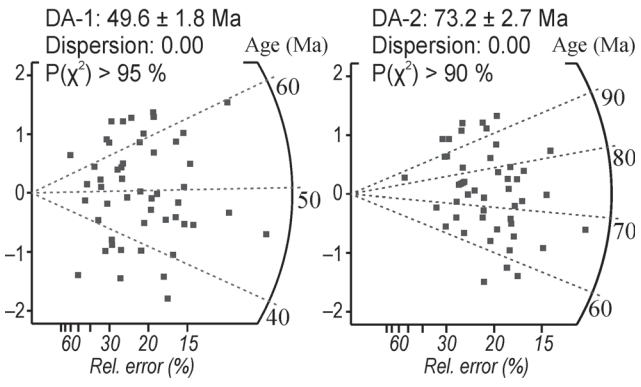

Fig. 3. Radial plots of the samples representing CCPB sediments.

7. Discussion

7.1 Thermal history modeling

As already advised in sections 6.2.1 and 6.2.2, the measured AFT ages are in fact geologically meaningless. But, it is possible to reveal their meaning by thermal modeling and to express the results in terms of time-temperature paths (or envelopes). It should be kept in mind that the thermal models are supposed to serve as a sort of test that can justify or dismiss presumptive hypotheses, so the modeling results should not be overestimated. Further, the modeling results are often strongly dependent on the skills of the modeler and the unavailability of other constraints on the thermal history results in too many acceptable solutions. Therefore the models should be constrained by as much information as possible.

In the following, we briefly review existing geological and thermochronological data that can help us to constrain the thermal evolution of the dated structural block.

The thermal model of the sedimentary samples DA-1 and DA-2 was constrained by their depositional age (T = 10–20 °C at ~33–26 and ~26–20 Ma, respectively) and that of the basement sample DA-3 by the ZFT age (T ≥ 210 °C at ~110–90 Ma) and by the age of exposure of the basement to the erosion level (T = 10–20 °C at ~20–15 Ma). The latter was inferred from the first occurrences of according detrital material in the Early? to Middle Miocene sequences in the neighbouring depressions (Gašparik et al. 1995; Hók et al. 1995, 1998).

Modeling was performed in the unsupervised search style. For all samples it revealed fairly similar tT paths (Fig. 4) with one conspicuous feature: all samples exhibit a distinct thermal event during the Middle Miocene, when they were suddenly reheated to temperature levels between ~60 °C and ~120 °C and afterwards cooled down to near-surface conditions. This thermal event coincides with the Middle Miocene volcanic activity in the region (~15–12 Ma) and affected the entire study area. This inference is also corroborated by the vitrinite reflectance data (R_O) from the Serravalian coal formation in the Handlová mine to the southeast of the Žiar Mts (for location see Fig. 1B). Petrík & Verbich (1995) reported R_O values from 0.28 up to 0.46 %, corresponding to maximum paleotemperatures of ~90–100 °C (Sweeney & Burnham 1990). The most obvious reasons for temperature increase were (i) mantle upwelling and/or (ii) magmatic activity producing large stratovolcanoes in the vicinity, as inferred from the multiple occurrences of volcanic material in the Neogene sedimentary record. The paleo-geothermal gradient in the Middle Miocene cannot be quantified, because there exist no AFT or vitrinite reflectance data from vertical profiles.

Although the AFT memory in the sedimentary samples was partially erased during the Miocene, it is still possible to get some information on the provenance of the samples. The thermal modeling revealed a fairly broad range of tT paths characterized by cooling between ~85 and ~50 Ma. Thus it can be concluded that the samples originated from a source area that cooled down through the apatite PAZ during Late Cretaceous to early Paleogene times. This interpretation is limited insofar the starting point in the thermal model could not be constrained by ZFT data.

The modeled cooling path of the basement sample suggests that, before reaching surface conditions in the Late Oligocene to Early Miocene, the basement cooled rapidly through the apatite PAZ between ~35 and ~25 Ma. Prior to this period of fast cooling, the basement was residing in

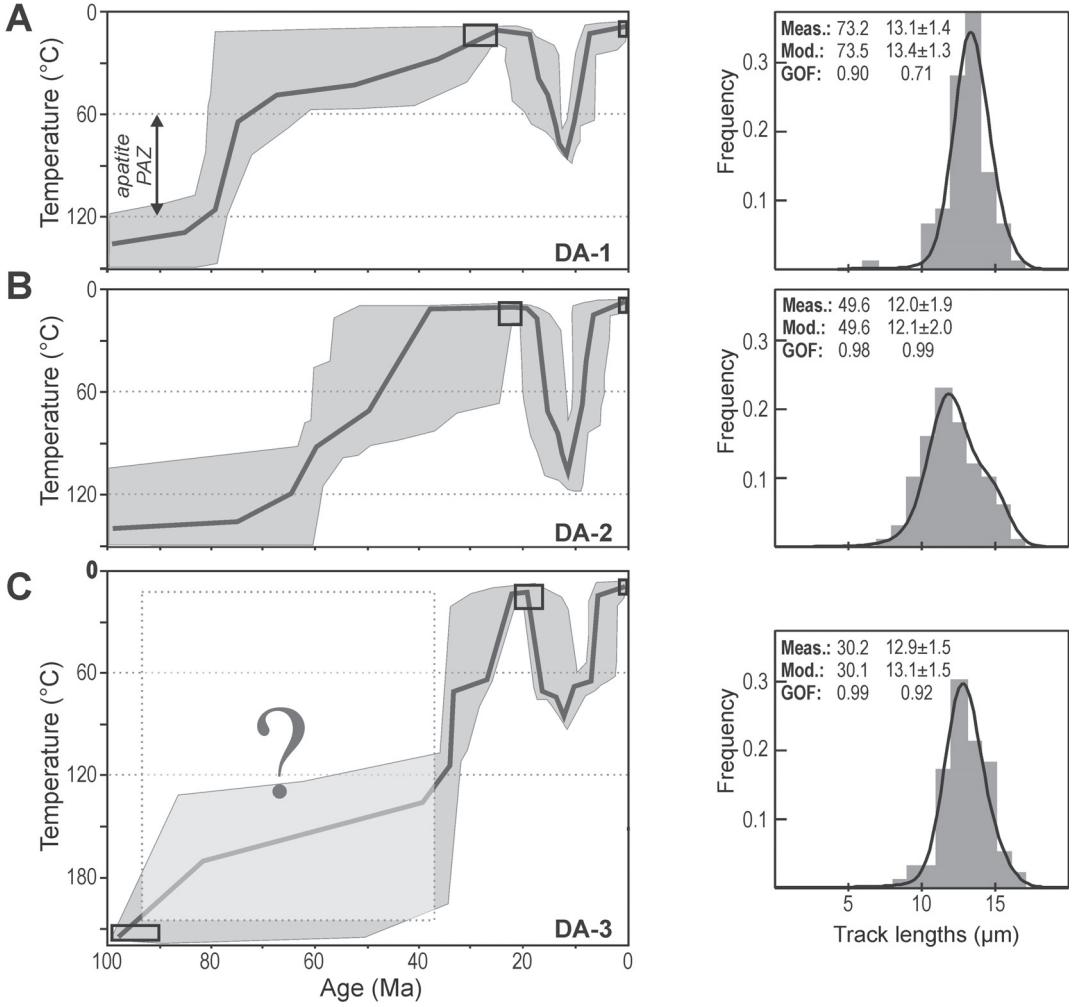

Fig. 4. Thermal modeling results of AFT data of the samples (**A, B** — sediment samples DA-1 and DA-2; **C** — basement sample DA-3) obtained with HeFTy program (Ketcham 2005). Results are displayed in time-temperature diagrams (left diagrams). Light grey envelopes — good fit; thick black line — best fit; black boxes — fixed constraints defined according to independent geological data. Right diagrams — frequency distribution of measured confined track length data overlain by a calculated probability density function (best fit). Meas. and Mod. — measured and modelled age in Ma (first numbers) and MTL ± SD in μm (second and third numbers), respectively; GOF — goodness of fit (statistical comparison of the measured input data and modeled output data, where a "good" result corresponds to value 0.5 or higher, "the best" result corresponds to value 1). Note that modeled tT paths are valid only inside the apatite PAZ, however outside this temperature range they must not necessarily represent the real thermal trajectory of a sample unless constrained by other data. For explanation of the field marked with question mark in the diagram C, see the text.

temperature conditions above ~120 °C so that the AFT system was totally reset. Therefore the cooling evolution of the basement in the period between the onset of fast cooling and the preceding mid-Cretaceous thermal event as fixed by the ZFT age cannot be reconstructed by thermal modeling alone (see the field marked with question mark in Fig. 4C). The simplest answer to the question what happened to the basement between 90 and 35 Ma was proposed by Kováč et al. (1994): after mid-Cretaceous thrusting and burial the basement cooled down in a moderate fashion from temperatures above ~210 °C to ~120 °C and remained there buried over a period of 60 Ma. There is, however, some evidence indicating that the basement must have been exposed to erosion after the thrusting and before the Paleogene transgression. For instance, Činčura & Köhler (1995) report Paleoalpine karstification of the Mesozoic carbonates during Late Cretaceous to early Paleogene times, when extensive parts of the IWC were exposed to subaerial weathering. Furthermore, there are abundant occurrences of Mesozoic rocks in the basal sequence of the Borové Formation of the CCPB (~50–39 Ma, Lutetian–Bartonian) showing that the Mesozoic nappes were eroded during that time. Most importantly, rare occurrences of granitic pebbles are reported from the Borové Formation near Ráztočno close to the Žiar Mts (Šimon et al. 1997). This signifies that even the granitoids of the basement were eroded prior to the transgression of the CCPB sediments.

Taking into consideration these arguments, we conclude that the basement was residing in near surface con-

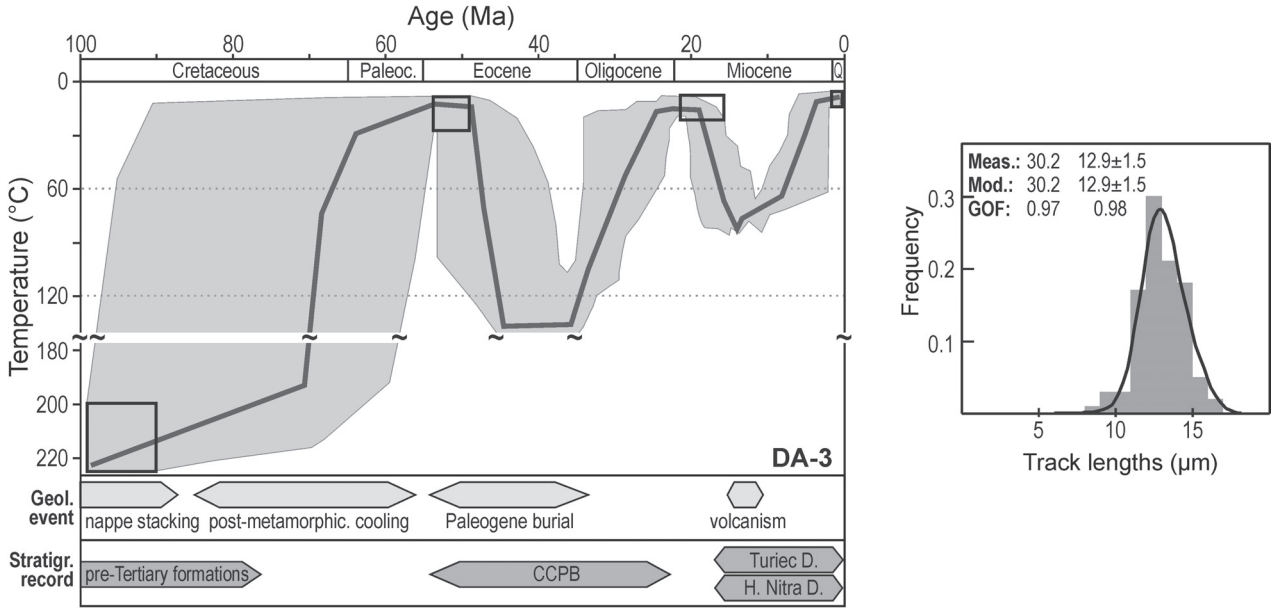

Fig. 5. Sumarizing time-temperature evolution of the crystalline basement drawn from regional geological considerations (main geological events and stratigraphic record preserved in the study area are depicted at the bottom of the left diagram) and from thermal modeling results of AFT data of the sample DA-3, constrained by an additional constraint (T = 10–30 °C at ~50 Ma, see text for explanation). For explanation of the diagrams see the caption of the previous figure.

ditions prior to the Paleogene transgression. Thus, the thermal model can be improved by an additional constraint (T = 10–30 °C at ~50 Ma). The resulting cooling path (Fig. 5) shows that the thermal event at ~110–90 Ma recorded by ZFT data was followed by a period of cooling, which might have occurred in a wide time span between ~100 and ~60 Ma. We interpret this post-metamorphic cooling event as a result of tectonic exhumation of the basement due to gravitational collapse and lateral extension of the nappe stack (Ratschbacher et al. 1989).

After residence in the surface levels in Late Cretaceous to early Paleogene times, the basement was reheated to temperatures sufficient to fully reset the AFT system (T ≥ 120 °C). We suggest that the period of heating was associated with the sedimentation in the CCPB, which developed at that time as a forearc basin in the Eastern Alps and IWC (Kázmér et al. 2003), and indicates that the basement was buried beneath a thick pile of sediments. Since the paleo-geothermal gradient in the Paleogene is not known, the amount of overburden can be estimated only indirectly: there is an indication that the CCPB formed in a cold crustal environment with low heat flow, as inferred from its fore-arc position (Kázmér et al. 2003) and from paleotemperatures as deduced from fluid inclusions (Hurai et al. 1995). Thus, we assume that the basement was buried by a ~8–12 km thick pile of CCPB sediments by using a gradient of ~10–15 °C/km.

Important implications from these conclusions are: (i) inspite of only sparse remnants, the entire area of the western IWC was buried by CCPB sediments in the Paleogene; (ii) during Paleogene, the geodynamic evolution of the western IWC was identical with that of the eastern IWC, where significant accumulations of CCPB sediments reaching up to 6 km are still preserved, and additional column of ~6 km has been eroded, as it is documented by fluid inclusion data (Hurai et al. 2000).

Another consequence is that the minimum age of the kaolin weathering crust in the Žiar Mts can be constrained more precisely. As mentioned in sections 2 and 2.1, it was proposed that the granitic batholith of the Žiar Mts emerged already in the Eocene — much earlier than the other granitic bodies of the Tatric belt. Therefore weathering of the granite commenced earlier and the kaolin weathering crust could develop to a higher maturation stage than anywhere else in the Tatric part of the IWC (Kraus 1989). However, our data clearly show that the batholith was still buried by sediments until middle Oligocene times, and weathering could therefore have started only after erosion of the CCPB sediments and exhumation of the basement. This happened probably during the Late Oligocene–earliest Miocene time as can be inferred from (i) the stratigraphic record — the youngest CCPB member preserved in the study area is of Chattian–Aquitanian age; (ii) the thermal modeling results — suggesting cooling associated with exhumation of the basement after inversion and erosion of the CCPB. From the Early to Middle Miocene, the basement must have been residing in near-surface conditions, forming a slightly undulating, low-relief surface favourable for supergene kaolinization. The period of kaolinization was terminated in the late Middle Miocene by tectonic activity causing vertical movements of tectonic blocks and creating the present horst-and-graben structure of the study area (e.g. Nemčok & Lexa 1990). The basement of the Žiar Mts was uplifted and largely eroded, as documented by occurrences of coarse crystalline pebbles and redeposited remnants of the kaolin

weathering crust in the Serravalian to Tortonian sequence of the Turiec Depression (Gašparik et al. 1974; Gašparik 1985; Kraus 1989).

8. Conclusions

The new fission track data combined with geological evidence allow us to improve the thermal history of the Žiar Mts and to draw the following conclusions:

— The Variscan crystalline basement of Žiar Mts experienced a complex thermal evolution characterized by post-metamorphic cooling and two periods of reheating — (i) during the Eocene and (ii) during the Middle Miocene.

— During the middle Cretaceous (~110–90 Ma) compressional tectonics, the crystalline basement of the Žiar Mts was overridden by Mesozoic nappes, buried to a depth with temperatures between ~210 °C and ~310 °C, and metamorphosed at least in anchizonal conditions, as documented by ZFT and Ar/Ar data. The crystalline basement thus records an Eo-Alpine overprint.

— The mid-Cretaceous thermal event was followed by a period of fast cooling of the basement through the apatite PAZ to near-surface conditions, as indicated by modeling results; we relate this cooling process to tectonic exhumation of the basement due to gravitational collapse and lateral extension of the nappe stack.

— In Late Paleocene–Early Eocene times, the emerged basement was progressively buried by sediments of the CCPB. During maximum burial the basement was reheated to temperatures above ~120 °C, indicating that the original thickness of Paleogene sedimentary column reached several kilometers in the study area. Thus we conclude that a thick pile of CCPB sediments covered the western part of the IWC.

— In the Late Oligocene to Early Miocene, the basement of the Žiar Mts was exhumed; the CCPB was disintegrated and inverted, most of the sediments were eroded. The minimum age of the kaolin weathering crust in the Žiar Mts must be Late Oligocene–Early Miocene, as inferred from the stratigraphy and AFT data.

— During the Middle Miocene, the samples from the basement and from the CCPB were reheated to temperatures between ~60 °C and ~120 °C, as recorded by the AFT data. This thermal event is related to the increased heat flow induced by upwelling of hot mantle material and related volcanic activity.

Acknowledgments: The German Science Foundation (DFG) funded this study. We would like to thank J. Kuhlemann (Tübingen) for assistance in the field and I. Kraus (Bratislava) for providing valuable information on the kaolin weathering in the Western Carpathians. Constructive reviews of the manuscript by Harald Fritz (Graz), Franz Neubauer (Salzburg) and Dušan Plašienka (Bratislava) are gratefully acknowledged. Gerlinde Höckh, Dorothea Mühlbayer-Renner and Dagmar Kost (Tübingen) are appreciated for careful sample preparation.

Appendix

Analytical procedure

Apatite and zircon crystals were recovered from whole-rock samples using standard magnetic and heavy liquid separation techniques. Apatites were embedded in epoxy, zircons in PFA Teflon^{TM}. Prepared mounts with grains were polished to 4π geometry. Spontaneous fission tracks in apatites were revealed by etching with 5.5 M HNO_3 solution for 20 seconds at 21 °C (Carlson et al. 1999; Donelick et al. 1999). Zircons were etched in an eutectic mixture of KOH and NaOH at 215 °C for 20 to 80 hours (Zaun & Wagner 1985).

Uranium contents of the samples were assessed by irradiating with thermal neutrons, which induce fission in a proportion of ^{235}U sample atoms. The induced tracks were recorded in an external detector of low-uranium muscovite sheets (Goodfellow mica^{TM}), attached to the sample during irradiation (Gleadow 1981). Samples were irradiated in the thermal column of the TRIGA nuclear reactor at Oregon State University, Oregon, USA, where the Cd ratio is ~14 which is well-suited to FT use. In the thermal facility, the reference value of neutron flux at the face (fully inserted) is 8×10^{10} n/cm^2/sec; the flux gradient is approximately 2 % per cm. Neutron fluence was monitored using Corning glass dosimeters CN-2 (for zircons) and CN-5 (for apatites), with a known uranium content of 37 ppm and 12 ppm, respectively (Hurford & Green 1982). Requested neutron flux for apatite samples was 4.5×10^{15} n/cm^2 and 1.5×10^{15} n/cm^2 for zircon samples. The apatite and zircon samples were irradiated for ~16 and ~5 hours, respectively.

After irradiation, mica detectors were etched in 40% HF for 30 minutes at 21 °C. Finally, the mounts with corresponding micas were attached side by side on a glass slide. Spontaneous ^{238}U and induced ^{235}U fission tracks were counted under the Zeiss Axioskop 2, equipped with a digitizing tablet, red LED cursor, drawing tube attachment, and controlled by the computer program FT Stage version 3.11 (Dumitru 1993). Tracks in apatites and mica-detectors were counted with 1250× magnification using dry objective, tracks in zircons were counted under the same condition but using oil immersion (Cargille oil type B, n = 1.515). Only crystals with well-polished surface parallel to the crystallographic c-axis and homogeneous uranium distribution were analysed, regardless of track density. The minimum of 25 grains from crystalline rocks and 50 grains from sediments were counted. Lengths of horizontal confined tracks and Dpars in apatites were measured only on grains oriented parallel to the crystallographic c-axis. A total of 100 horizontal confined tracks per sample were measured in order to obtain a representative and statistically robust distribution.

The IUGS-recommended zeta calibration approach was used to determine the ages (Hurford & Green 1983). The zeta value of 322.7 ± 5.3 for dosimeter glass CN-5 and 123.6 ± 2.1 for dosimeter glass CN-2 has been derived by analyst M. Danišík from 13 determinations of apatites and 9 of zircons from the Fish Canyon Tuff, Durango, and Tardree Rhyolite (Hurford 1998). FT ages were calculated with program TrackKey version 4.2 (Dunkl 2002).

Thermal history modeling based on AFT data

Modeling of the low-temperature thermal history based on AFT data was carried out using the HeFTy modeling program (Ketcham 2005). An inverse Monte Carlo algorithm with multi-kinetic annealing model (Ketcham et al. 1999) was used to generate tT paths. The annealing kinetics of apatite fission tracks was assessed by measurement of Dpar values. The input parameters we used in this study are the following: the central FT age with 1σ error; track length distribution (c-axes projected after Ketcham 2003); kinetic

parameter: Dpar values; the initial mean track length was estimated from Dpar and c-axis projected track lengths; the end of the tT path was set to 10 °C according to present-day mean surface temperature. Known geological information such as stratigraphic age of sedimentary samples or ZFT data measured on the same samples were converted into time-temperature constraints in the form of boxes. The tT paths were modeled in unsupervised search style.

References

Andriesen P.A.M. 1990: Anomalous fission track apatite ages of the Precambrian basement in the Hunnedalen region, south-western Norway. *Nucl. Tracks Radiat. Meas.* 17, 285–291.

Biely A. 1989: The geological structure of the West Carpathians. In: Rakús M., Dercourt J. & Nairn A.E.M. (Eds.): Evolution of the northern margin of Tethys. *Mém. Soc. Géol. France*, *Nouvelle Série* No. 154 (II), Paris, 51–57.

Bigazzi G. 1981: The problem of the decay constant of ^{238}U. *Nucl. Tracks* 5, 35–44.

Burtner R.L., Nigrini A. & Donelick R.A. 1994: Thermochronology of Lower Cretaceous source rocks in the Idaho-Wyoming thrust belt. *AAPG Bull.* 78, 10, 1613–1636.

Carlson W.D., Donelick R.A. & Ketcham R.A. 1999: Variability of apatite fissiontrack annealing kinetics I: Experimental results. *Amer. Mineralogist* 84, 1213–1223.

Crowley K.D., Cameron M. & Schaeffer R.L. 1991: Experimental studies of annealing of etched fission tracks in fluorapatite. *Geochim. Cosmochim. Acta* 55, 1449–1465.

Činčura A. & Köhler E. 1995: Paleoalpine karstification — the longest paleokarst period in the Western Carpathians (Slovakia). *Geol. Carpathica* 46, 6, 343–347.

Danišík M., Dunkl I., Putiš M., Frisch W. & Kráľ J. 2004: Tertiary burial and exhumation history of basement highs along the NW margin of the Pannonian Basin — an apatite fission track study. *Austrian J. Earth Sci.* 95, 96, 60–70.

Dodson M.H. 1973: Closure temperatures in cooling geochronological and petrological systems. *Contr. Mineral. Petrology* 40, 259–274.

Donelick R.A., Ketcham R.A. & Carlson W.D. 1999: Variability of apatite fission-track annealing kinetics: I. Experimental results. *Amer. Mineralogist* 84, 1224–1234.

Dumitru T.A. 1993: A new computer-automated microscope stage system for fission-track analysis. *Nucl. Tracks Radiat. Meas.* 21, 575–580.

Dunkl I. 2002: TRACKKEY: a Windows program for calculation and graphical presentation of fission track data. *Computers and Geosciences* 28, 2, 3–12.

Dunkl I., Frisch W. & Grundmann G. 2003: Zircon fission track thermochronology of the southeastern part of the Tauern Window and the adjacent Austroalpine margin. *Eclogae Geol. Helv.* 96, 209–217.

England P. & Molnar P. 1990: Surface uplift, uplift of rocks, and exhumation of rocks. *Geology* 18, 1173–1177.

Fendek M., Gašparik J., Gross P., Jančí J., Kohút M., Kráľ J., Kullmanová A., Planderová E., Raková J., Rakús M., Snopková P., Tuba Ľ., Vass D. & Vozárová A. 1990: Report on the research geothermal borehole ZGT-3 Turiec in Martin — Prognosis sources of the geothetmal energy in the area of Martin. *Open file report GÚDŠ*, Bratislava, 1–86 (in Slovak).

Frisch W. & Gawlick H.J. 2003: The nappe structure of the central Northern Calcareous Alps and its disintegration during Miocene tectonic extrusion — a contribution to understand the orogenic evolution of the Eastern Alps. *Int. J. Earth Sci.* 92, 712–727.

Galbraith R.F. & Laslett G.M. 1993: Statistical models for mixed fission track ages. *Nucl. Tracks Radiat. Meas.* 21, 459–470.

Gašparik J. 1985: The basic outlines of geological structure of the Horná Nitra and Turiec depression. In: Samuel O. & Franko O. (Eds.): Guide to XXVth National Geological Congress of the Slovak Geological Society. *GÚDŠ*, Bratislava, 53–56 (in Slovak).

Gašparik J., Brestenská E., Forgáč J., Franko O., Hajósová M., Hanáček J., Marková M., Matkulčík E., Planderová E. & Sitár V. 1974: Structural borehole GHŠ-1 (Horná Štubňa). *Region. Geol. Západ. Karpát* 3, 1–97 (in Slovak).

Gašparik J., Halouzka R., Miko O., Gorek J., Rakús M., Bujnovský A., Lexa J., Panáček A., Samuel O., Gašpariková V., Planderová E., Snopková P., Fendek M., Hanáček J., Modlitba I., Klukanová A., Žáková E., Horniš J. & Ondrejičková A. 1995: Explanations to geological map of the Turiec depression in a scale 1:50,000. *GÚDŠ*, Bratislava, 1–191 (in Slovak).

Gleadow A.J.W. 1981: Fission-track dating methods: what are the real alternatives? *Nucl. Tracks Radiat. Meas.* 5, 1, 2, 3–14.

Gleadow A.J.W. & Fitzgerald P.G. 1987: Tectonic history and structure of the Transantarctic Mountains: New evidence from fission track dating in the Dry Valleys area of southern Victoria Land. *Earth Planet. Sci. Lett.* 82, 1–14.

Gleadow A.J.W., Duddy I.R. & Lovering J.F. 1983: Fission track analysis: A new tool for the evaluation of thermal histories and hydrocarbon potential. *APEA Journal* 23, 93–102.

Gleadow A.J.W., Duddy I.R. & Green P.F. 1986a: Fission track lengths in the apatite annealing zone and the interpretation of mixed ages. *Earth Planet. Sci. Lett.* 78, 245–254.

Gleadow A.J.W., Duddy I.R. & Green P.F. 1986b: Confined fission track lengths in apatite: a diagnostic tool for thermal history analysis. *Contr. Mineral. Petrology* 94, 405–415.

Green P.F., Duddy I.R., Laslett G.M., Hegarty K.A., Gleadow A.J.W. & Lovering J.F. 1989: Thermal annealing of fission tracks in apatite 4: Quantitative modeling techniques and extension to geological timescales. *Chem. Geol.* 79, 155–182.

Gross P., Köhler E. & Samuel O. 1984: New lithostratigraphic classification of the Central Carpathians Paleogene. *Geol. Práce Spr.* 81, 103–117 (in Slovak).

Harrison T.M., Duncan I. & McDougall I. 1985: Diffusion of ^{40}Ar in biotite: Temperature, pressure and compositional effects. *Geochim. Cosmochim. Acta* 49, 11, 2461–2468.

Hók J., Šimon L., Kováč P., Elečko M., Vass D., Halmo J. & Verbich F. 1995: Tectonics of the Hornonitrianska kotlina Depression during the Neogene. *Geol. Carpathica* 46, 191–196.

Hók J., Kováč M., Rakús M., Kováč P., Nagy A., Kováčová-Slamková M., Sitár V. & Šujan M. 1998: Geologic and tectonic evolution of the Turiec depression in the Neogene. *Slovak Geol. Mag.* 4, 165–176.

Hurai V., Širáňová V., Marko F. & Soták J. 1995: Hydrocarbons in fluid inclusions from quartz-calcite veins hosted in Paleogene flysch sediments of the Central Western Carpathians. *Miner. Slovaca* 27, 383–396 (in Slovak, English summary).

Hurai V., Świerczewska A., Marko F., Tokarski A. & Hrušecký I. 2000: Paleofluid temperatures and pressures in Tertiary accretionary prism of the Western Carpathians. *Slovak. Geol. Mag.* 6, 2–3, 194–197.

Hurford A.J. 1986: Cooling and uplift patterns in the Lepontine Alps South Central Switzerland and age of vertical movement on the Insubric fault line. *Contr. Miner. Petrology* 92, 413–427.

Hurford A.J. 1998: ZETA: the ultimate solution to fission-track analysis calibration or just an interim measure. In: Van den haute P. & De Corte F. (Eds.): Advances in fission-track geochronology. *Kluwer Academic Publishers*, Dordrecht, 19–32.

Hurford A.J. & Green P.F. 1982: A user's guide to fission-track dating calibration. *Earth Planet. Sci. Lett.* 59, 343–354.

Hurford A.J. & Green P.F. 1983: The zeta age calibration of fis-

sion-track dating. *Chem. Geol.* 41, 285–312.

Kázmér M., Dunkl I., Frisch W., Kuhlemann J. & Ozsvárt P. 2003: The Palaeogene forearc basin of the Eastern Alps and the Western Carpathians: subduction erosion and basin evolution. *J. Geol. Soc.* 160, 413–428.

Ketcham R.A. 2003: Observations on the relationship between crystallographic orientation and biasing in apatite fission-track measurements. *Amer. Mineralogist* 88, 817–829.

Ketcham R.A. 2005: Forward and inverse modeling of low-temperature thermochronometry data. In: Reiners P.W. & Ehlers T.A. (Eds.): Low-temperature thermochronology: techniques, interpretations, and applications. *Rev. Mineral. Geochem.* 58, 275–314.

Ketcham R.A., Donelick R.A. & Carlson W.D. 1999: Variability of apatite fission-track annealing kinetics: III. Extrapolation to geologic time scales. *Amer. Mineralogist* 84, 1235–1255.

Kohút M. 1999: Study locality No. 3.2 — Žiar Mountains — Geological map and geological setting. In: Kováčik M. (Ed.): The selection of locality for Deep repository of radioactive waste in Slovakia. *Open file report*, *Slovenské elektrárne a.s. & ŠGÚDŠ*, Bratislava, 1–11 (in Slovak).

Kohút M., Madarás J., Žáková E., Marsina K. & Kováčik M. 2004: Geological evaluation of the structural borehole RAO-4 (Žiar). *Geol. Práce Spr., ŠGÚDŠ*, Bratislava, 51–60 (in Slovak).

Kováč M., Kráľ J., Márton E., Plašienka D. & Uher P. 1994: Alpine uplift history of the Central Western Carpathians: geochronological, paleomagnetic, sedimentary and structural data. *Geol. Carpathica* 45, 83–96.

Kováčiková M., Ondrášik M., Kováčik M. & Jetel J. 1995: Site selection methodology for deep repository of radioactive waste and prospective sites in Slovakia. *Slovak Geol. Mag.* 3, 191–200.

Kráľ J. & Štarková D. 1995: $^{40}Ar/^{39}Ar$ dating of selected minerals from the crystalline basement of the Tatricum and Veporicum. *Open file report ŠGÚDŠ*, Bratislava, 1–48 (in Slovak).

Kraus I. 1989: Kaolins and kaolinite clays of the Western Carpathians. *Západ. Karpaty. Sér. Mineral. Petrogr. Geochém. Metalogen. GÚDŠ,* Bratislava, 1–287 (in Slovak, English summary).

Laslett G.M., Green P.F., Duddy I.R. & Gleadow A.J.W. 1987: Thermal annealing of fission tracks in apatite 2. A quantitative analysis. *Chem. Geol.* 65, 1–13.

Lexa J. & Konečný V. 1998: Geodynamic aspects of the Neogene to Quaternary volcanism. In: Rakús M. (Ed.): Geodynamic development of the Western Carpathians. *GSSR*, Bratislava, 219–240.

Lexa J., Bezák V., Elečko M., Eliáš M., Konečný V., Less Gy., Mandl G.W., Mello J., Pálenský P., Pelikán P., Polák M., Potfaj M., Radocz Gy., Rylko W., Schnabel G.W., Stráník Z., Vass D., Vozár J., Zelenka T., Bilely A., Császár G., Čtyroký P., Kaličiak M., Kohút M., Kovacs S., Mackiv B., Maglay J., Nemčok J., Nowotný A., Pentelényi L., Rakús M. & Vozárová A. 2000: Geological map of Western Carpathians and adjacent areas 1:500,000. *ŠGÚDŠ,* Bratislava.

Maheľ M. 1986: Geological structure of the Czechoslovak Carpathians. Paleoalpine units. *Veda Publishing House*, Bratislava, 1–496 (in Slovak).

McDougall I. & Harrison T.M. 1988: Geochronology and thermochronology by the $^{40}Ar/^{30}Ar$ Method. *Oxford*, New York, 1–212.

Naeser N.D. 1992: Miocene cooling in the southwestern Powder River basin, Wyoming; preliminary evidence from apatite fission-track analysis. *USGS Bull.* 1917-O, 1–17.

Naeser N.D., Naeser C.W. & McCulloh T.H. 1989: The application of fission-track dating to the depositional and thermal history of rocks in sedimentary basins. In: Naeser N.D. & McCulloh T.H. (Eds.): Thermal history of sedimentary basins. *Springer-Verlag*, New York, 157–180.

Nemčok M. & Lexa J. 1990: Evolution of the basin and range structure around the Žiar mountain range. *Geol. Zbor. Geol. Carpath.* 41, 3, 229–258.

Petrík F. & Verbich F. 1995: The coal-petrology evaluation of the coal samples from the Handlová–Nováky coal basin. *Spravodaj BV* 4, 208–211 (in Slovak).

Plašienka D. 1997: Cretaceous tectonochronology of the Central Western Carpathians (Slovakia). *Geol. Carpathica* 48, 99–111.

Plašienka D., Grecula P., Putiš M., Kováč M. & Hovorka D. 1997: Evolution and structure of the Western Carpathians: an overview. In: Grecula P., Hovorka D. & Putiš M. (Eds.): Geological evolution of the Western Carpathians. *Miner. Slovaca Monograph*, Bratislava, 1–24.

Price P.B. & Walker R.M. 1963: Fossil tracks of charged particles in mica and the age of minerals. *J. Geophys. Res.* 68, 4847–4862.

Ratschbacher L., Frisch W., Neubauer F., Schmid S.M. & Neugebauer J. 1989: Extension in compressional orogenic belts: The eastern Alps. *Geology* 17, 404–407.

Ratschbacher L., Merle O., Davy P. & Cobbold P. 1991a: Lateral extrusion in the eastern Alps. 1. Boundary conditions and experiments scaled for gravity. *Tectonics* 10, 245–256.

Ratschbacher L., Frisch W., Linzer H.-G. & Merle O. 1991b: Lateral extrusion in the eastern Alps. 2. Structural analysis. *Tectonics* 10, 257–271.

Ring U., Brandon M.T., Willett S. & Lister G.S. 1999: Exhumation processes. In: Ring U., Brandon M.T., Lister G.S. & Willett S. (Eds.): Exhumation processes: Normal faulting, ductile flow and erosion. *Geol. Soc. Spec. Publ., London* 154, 1–28.

Stüwe K. 2002: Geodynamics of the lithosphere. *Springer*, New York, 1–449.

Stüwe K. & Barr T.D. 1998: On uplift and exhumation during convergence. *Tectonics* 17, 80–88.

Sweeney J.J. & Burnham A.K. 1990: Evaluation of a simple model of vitrinite reflectance based on chemical kinetics. *AAPG Bull.* 74, 1559–1670.

Šimon L., Elečko M., Gross P., Kohút M., Miko O., Pristaš J., Lexa J., Mello J., Hók J., Macínska M., Köhler E., Jánová V., Raková J., Snopková P., Samuel O., Stolár M., Vozár J., Kováč P., Vass D., Marcin D., Ďurkovičová J., Sládková M. & Wiegerová V. 1994: Explanations to geological maps 1:25,000, sheets: 36–133 (Handlová), 35–244 (Prievidza) & 36–131 Ráztočno. *Open file report, GÚDŠ,* Bratislava, 1–227 (in Slovak).

Šimon L., Elečko M., Pristaš J., Lexa J., Konečný V., Kohút M., Gross P., Halouzka R., Mello J., Polák M., Vozárová A., Vozár J., Havrila M., Stolár M., Jánová V., Köhlerová M., Marcin D. & Szalaiová V. 1997: Explanations to geological map of the Vtáčnik and Horná Nitra in a scale 1:50,000. *Regional geological maps of Slovakia*, *Dionýz Štúr Publishers*, 1–281 (in Slovak, English summary).

Thöni M. & Jagoutz E. 1992: Some new aspects of dating eclogites in orogenetic belts: Sm-Nd, Rb-Sr, and Pb-Pb isotopic results from the Austroalpine Saualpe and Koralpe type-locality (Carinthia/Styria, southern Austria). *Geochim. Cosmochim. Acta* 56, 347–368.

Thöni M. & Miller Ch. 1996: Garnet Sm-Nd data from the Saualpe and the Koralpe (Eastern Alps, Austria): chronological and P-T constraints on the thermal and tectonic history. *J. Metamorph. Geology* 14, 453–466.

Wagner G.A. & Van den haute P. 1992: Fission-track dating. *Enke Verlag*, Stuttgart, 1–285.

Wagner G.A., Reimer G.M. & Jäger E. 1977: Cooling ages derived by apatite fission-track, mica Rb-Sr and K-Ar dating: the uplift and cooling history of the Central Alps. *Mem. Inst. Geol. Miner. Univers. Padova* 30, 1–27.

Zaun P. & Wagner G.A. 1985: Fission track stability in zircon under geological conditions. *Nucl. Tracks Radiat. Meas.* 10, 303–307.